

THROMBOSIS AND HEMOSTASIS

A systems approach to hemostasis: 1. The interdependence of thrombus architecture and agonist movements in the gaps between plateletsJohn D. Welsh,^{1,2} Timothy J. Stalker,¹ Roman Voronov,² Ryan W. Muthard,² Maurizio Tomaiuolo,¹ Scott L. Diamond,² and Lawrence F. Brass¹¹Department of Medicine and ²Department of Chemical and Biomolecular Engineering, University of Pennsylvania, Philadelphia, PA**Key Points**

- Thrombus formation and contraction alters local molecular transport, which regulates agonist distribution and platelet activation.
- Semaphorin 4D contact-dependent signaling increases platelet activation, but does not affect platelet packing or agonist transport.

Hemostatic thrombi develop a characteristic architecture in which a core of highly activated platelets is covered by a shell of less-activated platelets. Here we have used a systems biology approach to examine the interrelationship of this architecture with transport rates and agonist distribution in the gaps between platelets. Studies were performed in mice using probes for platelet accumulation, packing density, and activation plus recently developed transport and thrombin activity probes. The results show that intrathrombus transport within the core is much slower than within the shell. The region of slowest transport coincides with the region of greatest packing density and thrombin activity, and appears prior to full platelet activation. Deleting the contact-dependent signaling molecule, Sema4D, delays platelet activation, but not the emergence of the low transport region. Collectively, these results suggest a timeline in which initial platelet accumulation and the narrowing gaps between platelets create a region of reduced transport that facilitates local thrombin accumulation and greater platelet activation, whereas faster transport rates within the shell help to limit thrombin accumulation and growth of the core.

Thus, from a systems perspective, platelet accumulation produces an altered microenvironment that shapes thrombus architecture, which in turn affects agonist distribution and subsequent thrombus growth. (*Blood*. 2014;124(11):1808-1815)

Introduction

The hemostatic response balances the need to halt bleeding with the need to avoid inappropriate vascular occlusion. Recent reports of hemostatic thrombi formed *in vivo* have demonstrated that the extent of platelet activation within a growing thrombus is heterogeneous¹⁻⁵ and can result in a characteristic core-and-shell architecture. We have shown that the core region develops adjacent to the injury site and consists of fully activated, closely packed platelets that have undergone α -granule exocytosis, which allows them to be recognized by the appearance of the α -granule membrane protein, P-selectin, on their surface.³ The shell is a less stable region that coats the core and consists of loosely packed, less activated platelets.³

Regional differences in the extent of platelet activation can potentially be driven by multiple factors. Here we have adopted a systems biology perspective, looking beyond the events in any one platelet to test the idea that the emerging architecture of the hemostatic response serves as both a driver and a reflection of differences in intrathrombus molecular transport rates and consequent differences in agonist distribution. Numerous platelet agonists are present during vascular injury, including collagen, thrombin, adenosine 5'-diphosphate (ADP), and thromboxane A₂ (TxA₂).⁶ Each of these varies in origin, potency, and mobility. Collagen, for example, is immobile, whereas

thrombin distribution is limited by interactions with other proteins, including inhibitors.^{7,8} By comparison, ADP and especially TxA₂ are freely diffusible.⁹

Our goal in this study was to develop and apply methods to understand the relationship between molecular transport, platelet packing density, and agonist distribution, examining how each affects platelet activation and thrombus growth *in vivo*. We asked whether regional differences in thrombus structure affect agonist movement and distribution, and, therefore, the extent of platelet activation. To test this hypothesis, we developed a novel biosensor capable of measuring molecular transport *in vivo* in real time, and have used that biosensor in conjunction with a previously developed thrombin biosensor¹⁰ to compare transport rates and thrombin activity. The transport biosensor consists of albumin coupled to caged fluorescein molecules that uncage and fluoresce when flashed with 405-nm light. Subsequent loss of the fluorescence provides a direct measure of intrathrombus transport that we have combined with data generated by the thrombin biosensor and a thrombus porosity probe to produce a high-resolution map of transport rates, thrombin activity, and relative packing density within the thrombus.

Here we show for the first time that molecular transport in the gaps between platelets *in vivo* is orders of magnitude slower within the

Submitted January 25, 2014; accepted June 14, 2014. Prepublished online as *Blood* First Edition paper, June 20, 2014; DOI 10.1182/blood-2014-01-550335.

The online version of this article contains a data supplement.

There is an Inside *Blood* Commentary on this article in this issue.

The publication costs of this article were defrayed in part by page charge payment. Therefore, and solely to indicate this fact, this article is hereby marked "advertisement" in accordance with 18 USC section 1734.

© 2014 by The American Society of Hematology

thrombus than in the overlying blood stream, and even slower in the core than in the shell. High-resolution mapping defines a low transport region (LTR) coinciding with the region of greatest packing density and highest thrombin activity. Because greater packing density facilitates contact-dependent signaling between adjacent platelets, we performed comparative studies in mice lacking Sema4D. These mice have a defect in contact-dependent amplification of collagen-induced platelet activation.¹¹ Collectively, the results establish a timeline in which initial platelet accumulation and the narrowing gaps between platelets serve as obstacles to molecular movement in what will become the thrombus core. This creates a region of reduced transport that facilitates local thrombin accumulation and greater platelet activation, whereas faster transport rates and greater instability within the shell help to limit thrombin accumulation and thrombus size. Thus, even the early stages of platelet accumulation produce an altered microenvironment that influences subsequent thrombus growth and, potentially, the impact of antiplatelet agents. In this and the 2 accompanying manuscripts,^{12,13} we use complementary experimental and computational approaches to test this model.

Methods and materials

Materials

5-Carboxymethoxy-2-Nitrobenzyl (CMNB)-caged carboxyfluorescein succinimidyl ester (SE) and Alexa Fluor 488/568/647 monoclonal antibody labeling kits were obtained from Life Technologies. Bovine serum albumin (BSA) was obtained from Jackson Immunological Research. C57Bl/6J mice were obtained from The Jackson Laboratory. Anti-CD62P (IgG, clone RB40.34) and the anti-CD41 (F(ab)₂ fragment, clone MWRReg30) were obtained from BD Biosciences.

Synthesis of caged fluorescein conjugated to albumin (cAlb). BSA was solubilized in 0.1M sodium bicarbonate in phosphate-buffered saline to a final concentration of 10 mg/mL. CMNB-caged carboxyfluorescein SE was dissolved in 100 μ L of dimethyl sulfoxide, and added to the solubilized BSA and mixed thoroughly. The reaction was incubated for 1 hour at room temperature, and then excess caged fluorescein was removed using 7-kDa molecular weight cutoff desalting columns (Thermo Scientific).

Hemostatic thrombus formation

Male mice 8 to 12 weeks of age were anesthetized with an intraperitoneal injection of sodium pentobarbital (90 mg/kg), and their jugular vein was cannulated for the introduction of cAlb (0.5 mg/mL), anti-CD41 AF-568, and anti-CD62P AF-647. The mouse cremaster was exposed, cleaned of connective tissue, opened, and prepared for viewing by intravital microscopy. The cremaster was maintained under a constant flow of bicarbonate buffer (37°C) bubbled with 95%/5% N₂/CO₂. Mouse arterioles of 30- to 50- μ m diameter were visualized with a BX61WI microscope (Olympus) with a 60 \times (0.9 NA) water-immersion objective, and a CSU-X1 spinning disk confocal scanner (Yokogawa). Fluorescence imaging was done using diode pumped solid state lasers (405 nm, 488 nm, 561 nm, 647 nm) with acousto-optic tunable filter control as an excitation source (LaserStack; Intelligent Imaging Innovations), and images were captured using an Evolve digital camera (Photometrics). Endothelial cell ablation was performed with a pulsed nitrogen dye laser (SRS NL100, 440 nm) focused on the vessel wall through the microscope objective. The laser was fired between 1 and 10 times until red blood cells either escaped into the extravascular space or became trapped within the layers of the vessel wall. The University of Pennsylvania Institutional Animal Care and Use Committee approved all procedures.

Injury visualization

After injury, the platelet deposition was monitored using anti-CD41 AF-568 fluorescence, and core development with anti-P-selectin (anti-CD62P).

Background fluorescence was measured within the vessel for both anti-CD41 and anti-P-selectin, and subtracted from the images to determine the core and shell areas. In representative images of thrombi using anti-CD41, anti-P-selectin, and thrombin sensor, the background fluorescence threshold is set and the results are displayed in binary mode unless otherwise noted in the figure legend.

cAlb fluorescence was visualized by uncaging the caged carboxyfluorescein with a 500-ms pulse of 405-nm light delivered through the microscope objective (Figure 1A-B). Immediately after the 405-nm light pulse, cAlb fluorescence (excitation, 488 nm), platelets (excitation, 568 nm), and P-selectin (excitation, 647 nm) were tracked for 15 frames. After 15 frames (~9 seconds), a new pulse was initiated. This sequence was repeated for 3 minutes. Separate studies determined that the observed rapid decay is not due to photobleaching, as only very mild photobleaching was observed using the experimental capture settings (supplemental Figure 1, see supplemental Data available on the *Blood* Web site). Microscope control, image capture, and analysis was performed by Slidebook 5.0 (Intelligent Imaging Innovations).

Thrombin biosensor

Mouse thrombin-sensitive antibody (mThS-Ab) was synthesized using a protocol previously described.¹⁰ mThS-Ab was infused through the jugular cannula of the mouse prior to injury and was imaged every 10 seconds. Platelets and P-selectin were labeled with fluorescent anti-GPIIb/3 (clone Xia.C3; Emfret Analytics) and anti-CD62P, respectively, and were imaged once per second. Background fluorescence was measured within the vessel and subtracted from the mThS-Ab signal within the thrombus. Determining the location of the stable core at 20 minutes postinjury identified the LTR, and mThS-Ab was quantified within the LTR and shell over time.

Analysis of cAlb data

For core and shell cAlb decay rates, the core and shell were masked using P-selectin staining as the marker for core. For each mask, the cAlb decay curves were obtained once the region attained an area >10 μ m². The mean cAlb fluorescence intensity in the core and shell regions immediately prior to each 405-nm flash was defined as background fluorescence and subtracted from the cAlb images acquired subsequent to each flash. The mean cAlb fluorescence for each of the images acquired following each flash were then normalized to the cAlb fluorescence in the first image postflash (representing the peak cAlb signal for each flash), resulting in a decay curve for each 405-nm flash. All the curves for a single injury were averaged to make a single decay curve, and curves for multiple injuries were averaged to generate the mean curves with standard deviations reported. The curves were averaged over several injuries from at least 3 mice.

Sema4D-deficient mice backcrossed onto C57Bl/6 were described previously.¹⁴ All studies were performed using Sema4D^{+/+} (denoted as wild-type [WT]) and Sema4D^{-/-} littermates produced by crossing heterozygotes.

Porosity measurements

BSA labeled with Alexa Fluor 488 (Invitrogen) was infused into the mouse through a jugular cannula prior to injury. Fluorescence was measured continuously in the lumen, LTR, and shell during thrombus development. The lumen was assumed to have a porosity of 0.6 due to 40% hematocrit in the flowing blood, and the measured lumen fluorescence was used to calculate the plasma fluorescence with a porosity of 1. By normalizing the fluorescence within the shell and LTR to the plasma, we were able to calculate the porosity of each region over time.

Results

Measuring regional heterogeneity of intrathrombus transport

A necessary first step in this study was the development of a method to measure intrathrombus molecular transport rates in vivo in real

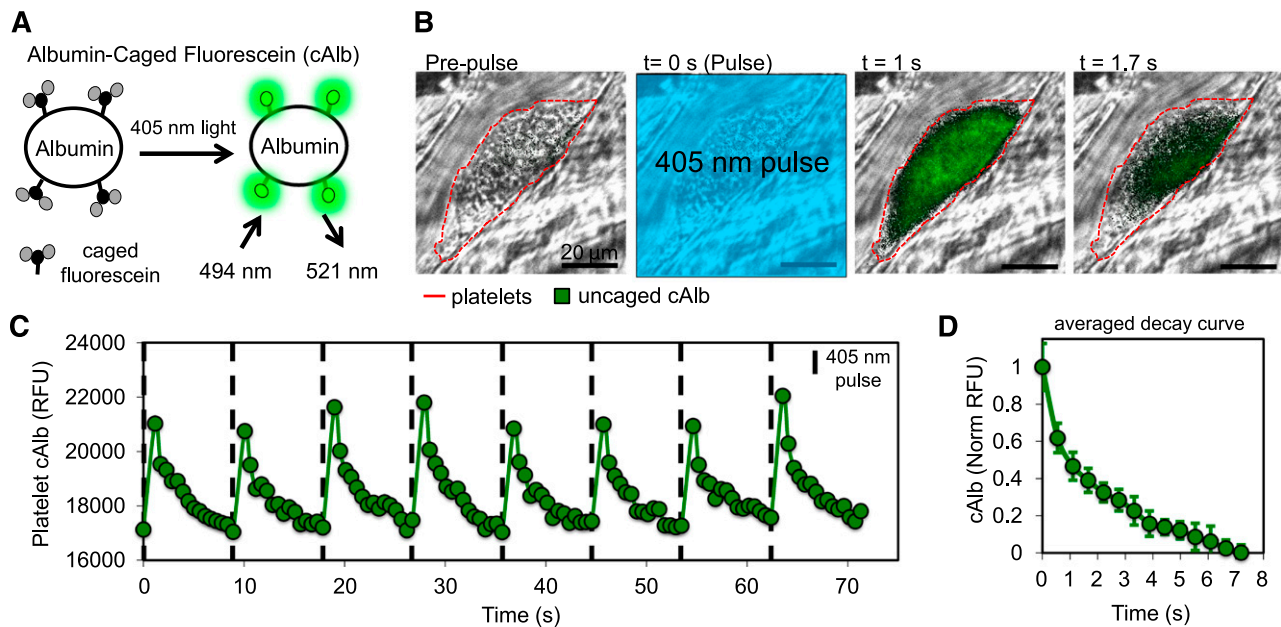


Figure 1. Design of cAlb biosensor for visualization of the molecular transport properties of thrombi generated in vivo. (A) BSA was labeled with cAlb, which is uncaged using 405-nm light to induce fluorescence. (B) Intravital microscopy was used to observe cAlb in vivo. Infusion of cAlb into the blood stream was followed by laser-induced injury to the mouse cremaster muscle arterioles to induce thrombus formation. Periodic pulses of 405-nm light were used to uncage cAlb and the resulting fluorescence intensity and decay were monitored with fluorescent microscopy. The represented fluorescence intensity has had the background subtracted and then been scaled to demonstrate signal decay within the thrombus. (C) Quantification of the intrathrombus cAlb signal was measured over multiple pulses of uncaging light for thrombus in panel B. (D) An average intrathrombus cAlb decay curve was generated by averaging the decay after each of 16 pulses taken over 3 minutes.

time during hemostatic thrombus formation. The injury model we have used most frequently uses a laser or sharpened glass probe to produce a penetrating injury in the cremaster muscle microcirculation of a C57Bl/6 mouse.³ Thus, in this and the 2 accompanying manuscripts, our focus is on the hemostatic response to injury and we have used the terms “hemostatic thrombus,” “hemostatic plug,” and “thrombus” interchangeably. Confocal fluorescence microscopy with high-speed video capture allows direct visualization of the response to injury and parameters such as platelet accumulation, platelet activation, packing density, and thrombus porosity to be measured, the latter with stably fluorescent albumin and dextran molecules.³ To create a transport rate sensor for the present studies, albumin was labeled with caged fluorescein molecules (cAlb) that become stably fluorescent only after being uncaged by exposure to 405-nm light (Figure 1A and supplemental Video 1). In the example shown in Figure 1B, pulses of 405-nm light uncaged the fluorophore within the field of view resulting in fluorescence that could be visualized within the thrombus. The rise and subsequent washout of fluorescence within the thrombus caused by a series of repeated light pulses separated by 10 seconds is shown in Figure 1C. Albumin-associated fluorescence in the lumen moves too rapidly for capture and analysis. Each thrombus was monitored for 3 minutes after injury, during which time multiple pulses and decay curves were generated (Figure 1D). Photobleaching contributed minimally to the decline in cAlb fluorescence during the period of observation between activating pulses (supplemental Figure 1). Platelet deposition and surface P-selectin expression (an index of α -granule exocytosis) were recorded at the same time (Figure 2A-B).

As reported previously, platelets accumulate rapidly in this injury model, reaching a peak 30 to 60 seconds after injury.³ Surface P-selectin appears more slowly, becoming detectable within the thrombus core at 20 seconds and continuing to increase throughout the experiment with growth slowing after \sim 150 seconds (Figure 2B). To determine whether molecular transport rates also show regional variation, cAlb decay was analyzed separately in the P-selectin(+)

core region and P-selectin(–) shell region of the thrombus. Average cAlb decay curves were generated for 13 injuries during the first 3 minutes postinjury for both regions (Figure 2C). We found that uncaged (ie, fluorescent) cAlb was visible only within the thrombi. cAlb in the lumen of the vessel was traveling too fast to be flash-activated and observed. The core region had an average cAlb half-life of 2.6 seconds, which is approximately twofold greater than the shell region’s average half-life of 1.2 seconds. Detailed mapping showed that the slowest half-life recorded in the core was 8 seconds and the fastest in the shell was 0.5 seconds, yielding a maximum ratio of 16:1. Taken together, these results demonstrate, first, that platelets retard the movement of soluble molecules in their vicinity and, second, the core and shell have differing transport properties, with the core-retaining soluble proteins longer than the shell.

Determining the kinetics of reduced intrathrombus transport and platelet packing

We hypothesized that slower molecular transport in the core leads to greater retention of soluble agonists, which in turn contributes to full platelet activation and α -granule secretion. If so, then reduced transport rates in the core region would precede P-selectin exposure on the platelet surface. To compare the kinetics of the development of regions of reduced transport with the kinetics of platelet activation, we identified a transition zone, defined as the region that is P-selectin(–) at 3 minutes, but becomes P-selectin(+) by 20 minutes (Figure 3A). Taking into account this definition of a transition zone, the shell region becomes the part of the thrombus that is neither core nor transition region. We found that the transition zone at 3 minutes postinjury, despite being P-selectin(–), had significantly slower cAlb transport than the shell (Figure 3B).

To generate a map of intrathrombus transport rates with the greatest possible resolution, we analyzed cAlb decay rates for single pixels within early thrombi (2–3 minutes postinjury), yielding high spatial-resolution cAlb $t_{1/2}$ heat maps for each

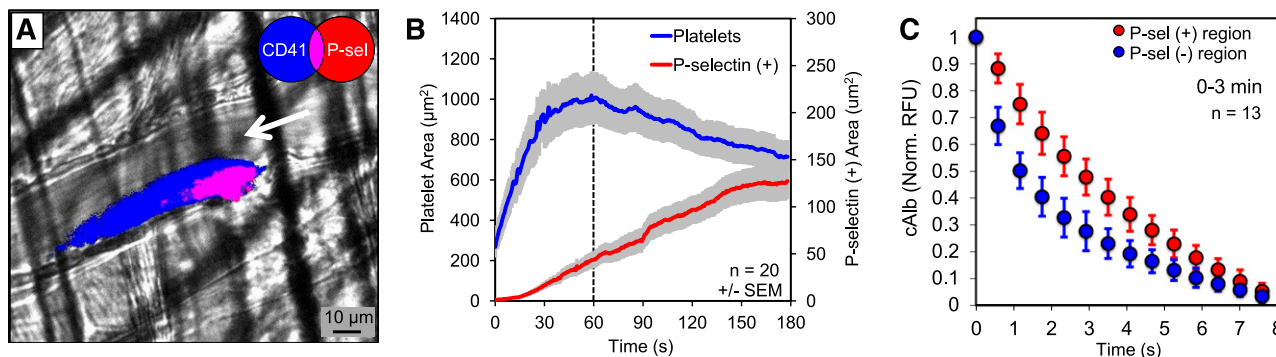


Figure 2. Regional heterogeneity of cAlb transport properties. (A) A representative image of a thrombus generated using a laser injury model in mouse cremaster arterioles (3 minutes postinjury). Thrombi were monitored for platelet deposition (blue), P-selectin exposure (red), and cAlb (not shown) for 0 to 3 minutes post-injury. (B) The growth of platelet (blue) and P-selectin(+) (red) areas were monitored over 3 minutes. The areas were measured by gating the images on either CD41(+) or P-selectin(+) pixels and then averaged across 20 injuries from 5 WT mice. (C) Thrombus regions were defined as CD41(+)/P-selectin(+) and CD41(+)/P-selectin(-) for cAlb analysis. Pulses of 405-nm light were used to activate the cAlb infused prior to injury, and the normalized decay curves for the P-selectin(+) (red) and P-selectin(-) (blue) regions were averaged over each pulse for 0 to 3 minutes postinjury (\pm SD).

thrombus (supplemental Methods, Figure 3C). We observed a gradient of cAlb half-lives extending from the region adjacent to the injury site showing the slowest transport. This region of low transport extended beyond the P-selectin(+) region into the transition zone (Figure 3C). Taken together the transition zone and the core form a LTR, which has significantly reduced transport compared with the shell region (Figure 3C-D). The appearance of reduced transport rates within the LTR preceding full platelet activation suggests a model in which transport heterogeneity regulates agonist distribution and platelet activation, which in turn affect platelet packing density and, therefore, local transport rates.

Measuring platelet packing dynamics within the LTR

Within stable thrombi, the core maintains a higher platelet packing density, resulting in significantly decreased porosity.³ We hypothesized

that this high-density structure produces lower transport rates in the core by increasing steric hindrance between platelets, reducing permeability, and by increasing the tortuosity of the path cAlb needs to traverse to escape the core. To measure the dynamics of the increase in platelet packing density during early thrombus development, we infused albumin conjugated with stably fluorescent (ie, not caged) Alexa Fluor 488 and monitored changes in fluorescence within the LTR and shell region. For reference, fluorescence was also measured outside of the thrombus in flowing blood, which consists of \approx 40% hematocrit and a porosity of 0.6. By normalizing the fluorescence within the thrombus regions to the known value of the flowing blood, we were able to determine the porosity of each region within the thrombus (Figure 4). We found that porosity decreases rapidly in both regions as platelets accumulate following injury, with the LTR achieving a significantly higher packing density than the shell by 60 seconds after injury ($P < .05$). As reductions in both porosity and

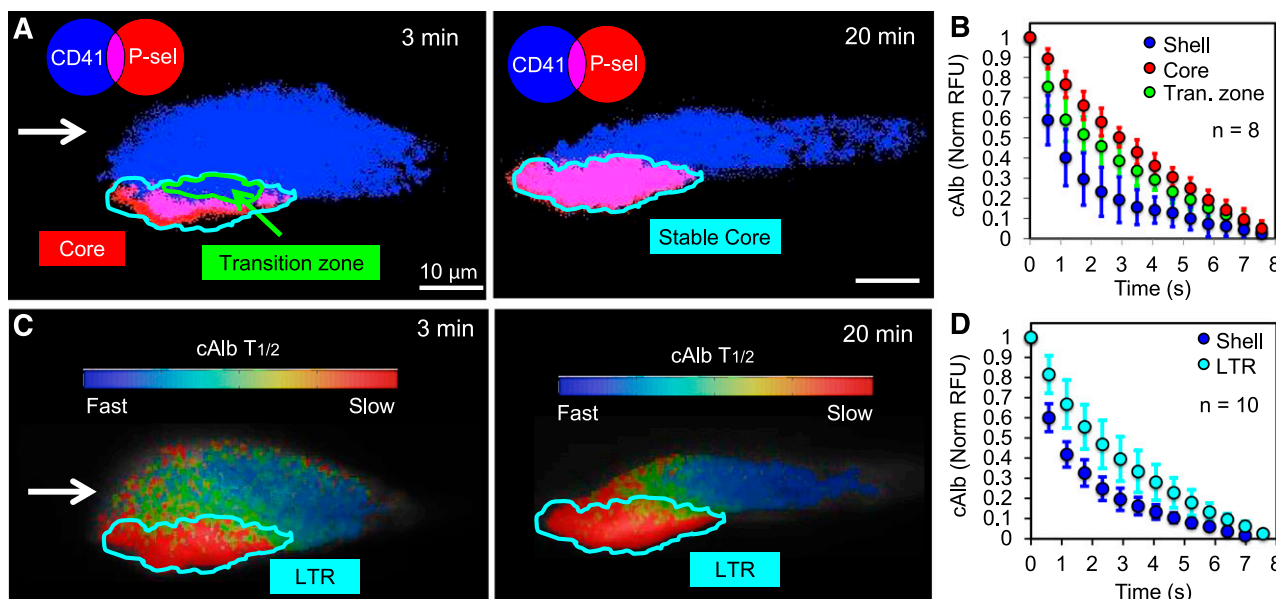


Figure 3. Transport properties of the transition zone. (A) A representative image of a thrombus at 3 minutes and 20 minutes postinjury showing platelet deposition (blue) and P-selectin exposure (red) at 3 minutes and 20 minutes. Also shown are the stable core (cyan outline) 20 minutes postinjury, and the transition zone (green outline) at 3 minutes postinjury. (B) Eight of the injuries had transition zones (green) large enough ($>10 \mu\text{m}^2$) to be analyzed in addition to the core (red) and shell (blue) regions for their average cAlb decay curves (\pm SD). (C) For those same images in panel A, the resulting cAlb $t_{1/2}$ time heat maps are shown with the LTR highlighted (cyan). The LTR is defined as the P-selectin(+) region plus the transition zone (ie, the P-selectin(+) region at 20 minutes postinjury). (D) Analysis of the LTR (cyan) transport compared with the shell (blue) transport properties using cAlb.

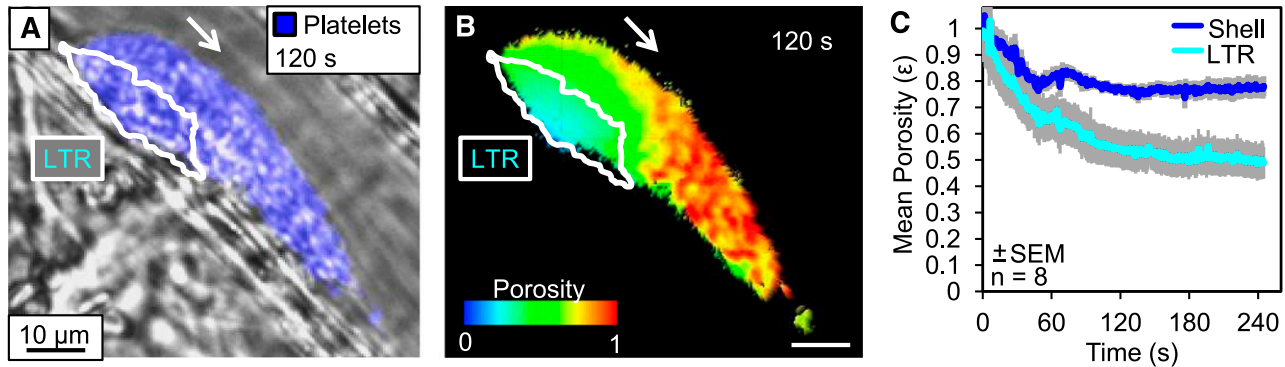


Figure 4. Dynamics of thrombus regional porosity. Albumin labeled with Alexa Fluor 488 was infused into the mouse prior to injury and the fluorescence was monitored within the lumen, LTR, and shell of the developing thrombi. (A) A representative image of platelets (blue) and LTR (white outline) 120 seconds postinjury. (B) For the same thrombus, a pseudo-colored image of the thrombus colored to represent the porosity based on the normalized fluorescence intensity. (C) Average porosity of the shell (blue) and LTR (cyan) of 8 individual injuries over 240 seconds postinjury.

transport are observed prior to full platelet activation, this also supports our model of transport having a regulatory role in local platelet activation.

Regional heterogeneity of intrathrombus thrombin activity

To determine whether the altered structure and transport of the LTR serve to concentrate agonists leading to increased platelet activation and eventual P-selectin exposure, we used a recently developed thrombin activity sensor, designated mThS-Ab. The thrombin sensor consists of a fluorescence resonance energy transfer–based fluorogenic peptide thrombin substrate linked to anti-mCD41 to target it to the platelet surface.¹⁰ Cleavage of the peptide by thrombin releases a quencher, allowing an increase in fluorescence. The resulting signal represents the spatial distribution of cumulative thrombin activity. Thrombin activity, platelet deposition, and P-selectin exposure were measured in developing (0–3 minutes after injury) and stable thrombi (20 minutes after injury) (Figure 5A and supplemental Video 2). Consistent with our previous observation that fibrin deposition occurs only within the core region,³ we measured 6.5 times more thrombin activity within the LTR than within the shell by 3 minutes after injury (Figure 5B). By 20 minutes even the minor signal in the shell was no longer detectable.

Determining pathways which initiate and support LTR formation

Because the data described so far show that the drop in transport rates within hemostatic thrombi precedes full platelet activation, we examined the effect of impairing platelet activation on transport rates. To do this, we selected *Sema4D*^{-/-} mice, whose signaling

defect we have characterized previously.^{11,14} *Sema4D* is a semaphorin family member on the surface of platelets that supports contact-dependent amplification of Syk activation downstream of the platelet collagen receptor, GPVI.¹¹ When studied after penetrating injury, *Sema4D*^{-/-} mice show a defect in platelet accumulation and delayed P-selectin exposure during the first 3 minutes of thrombus development.³ The studies in Figure 6 confirm this earlier observation. They also show that these mice have no significant defect in cAlb transport during this same period (Figure 6C–D). Thus, these results reinforce the idea that the drop in transport rates within the thrombus not only precedes full platelet activation (as defined in this case by α -granule exocytosis), but is at least partially independent of it.

Discussion

Studies in mouse models reveal that rather than being a homogeneous mass of equally activated platelets uniformly interspersed with fibrin, the hemostatic response to penetrating injuries shows considerable regional variation in the extent of platelet activation as judged by metrics such as the extent of α -granule exocytosis. In this and 2 accompanying manuscripts,^{12,13} we have adopted a systems approach to understanding these events, combining observational, experimental, and computational approaches to ask whether regional differences extend to other aspects of the hemostatic response and, if so, how such differences arise, contribute to thrombus growth, and affect the benefits and toxicities of antiplatelet agents.

To do this, we developed a novel tool for measuring intrathrombus transport rates in vivo in real time and combined it with a recently

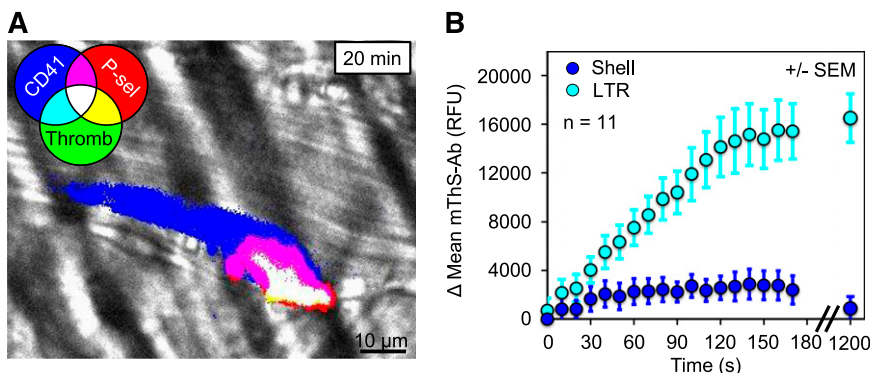


Figure 5. Thrombin activity within the LTR. (A) A representative image of thrombin activity (mThS-Ab; green, binary mode) within a thrombus 20 minutes after injury also showing platelet deposition (blue) and core formation (red). Overlay of 3 channels is white. (B) The change in the mean mThS-Ab fluorescence was monitored within the LTRs (cyan) and shell (blue) during the initial 3 minutes after injury and again at 20 minutes (\pm SEM).

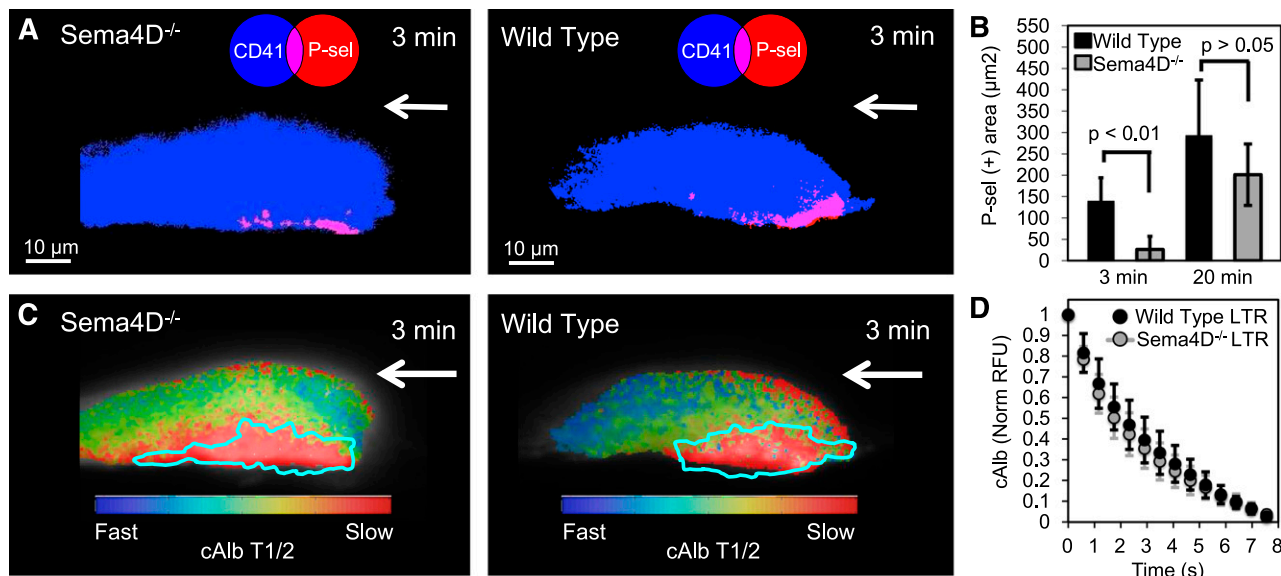


Figure 6. The role of contact-dependent Sema4D signaling in LTR and core formation. (A) Representative images of a thrombus generated in Sema4D^{-/-} and WT mice cremaster muscle arterioles showing platelets (blue) and P-selectin (red) at 3 minutes postinjury. (B) Quantification of the average P-selectin(+) area within Sema4D^{-/-} and WT thrombi at 3 and 20 minutes postinjury (n = 13 for both Sema4D^{-/-} and WT; ^{+/-} SD) showing a lag in P-selectin exposure in the knockout. (C) For each representative thrombus, the corresponding cAlb half-life heat map is shown with the LTR highlighted (cyan). (D) The cAlb decay curves of the LTR of wild-type (black) and Sema4D^{-/-} (gray) thrombi (WT, n = 10; Sema4D^{-/-}, n = 14; \pm SD).

described thrombin activity sensor.¹⁰ The results presented here show that regional differences in the extent of platelet activation are accompanied by differences in platelet packing density, intra-thrombus molecular transport rates, distribution of at least 1 platelet agonist (thrombin), and deposition of fibrin. The results also show how these relationships evolve over time (Figure 7). High-resolution mapping based on confocal in vivo imaging studies transforms the transport data into a heat map and defines a hitherto unappreciated transition zone between the thrombus core and shell. Within this zone are platelets that have not yet reached the point of α -granule exocytosis, but nonetheless retard the passage of solutes in the spaces between them. The transition zone plus the core of platelets that became P-selectin(+) early in the injury response form a LTR that eventually becomes fully P-selectin(+).

Changes in transport rates presumably reflect the increase in packing density as platelets grow closer to each other, increasingly hindering the movement of molecules in the gaps between platelets. Supporting this conclusion, we found that the distribution of thrombin activity within the thrombus mirrored the regions of slowest transport and extended little, if at all, into the shell region of the thrombus

where transport rates, although slower than in the remaining vascular lumen, were still faster than in the core. Data presented in an accompanying manuscript¹² provide further support, showing that mice with a defect in $\alpha_{IIb}\beta_3$ outside-in signaling that impairs clot retraction form thrombi with increased transport in both the core and the shell, and decreased thrombin activity compared with WT mice. Here we studied mice with a defect in contact-dependent signaling due to loss of the platelet surface ligand, Sema4D. These mice have a defect in core formation, but still developed an LTR, supporting the idea that the reduced transport is not dependent on achieving full platelet activation.

The close relationship between the LTR and the region of greatest thrombin activity is particularly informative. Others have also presented models suggesting that solute transport may play a key role in regulating thrombus growth by impacting coagulation factor access to the injury site as well as agonist escape from the thrombus.^{15,16} These models have shown that limiting the gaps between platelets can greatly hinder transport and alter the movement of solutes through the thrombus.¹⁵⁻¹⁷ Within this study we were unable to tease apart the contribution of fibrin in filling these gaps,

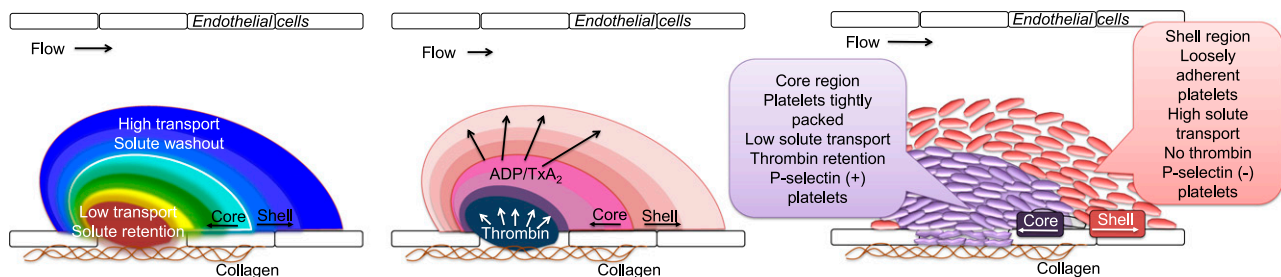


Figure 7. Model of the role of transport on agonist distribution and thrombus architecture. As platelets within a developing thrombus become activated, they change shape, retract, and pack tightly together driving the formation of the LTR. This leads to the retention of larger agonists, such as thrombin, within the LTR. Smaller agonists, such as ADP and TxA₂, are able to diffuse more freely out of the LTR. The localization of these agonist gradients drives continued platelet activation in the LTR leading to core formation consisting of high platelet packing density, decreased solute transport, α -granule exocytosis, and fibrin deposition. The restriction of thrombin to the core contributes to the shell consisting of loosely adherent platelets, high solute transport, reduced platelet activation, and no fibrin.

but other investigators¹⁸ have suggested fibrin does not have a large impact on protein diffusive transport. However, fibrin has been reported to decrease the permeability of platelet plugs,¹⁹ which may alter permeating flow and in turn protein transport.

We have previously shown that thrombin inhibitors prevent the formation of the core region.³ Generation of thrombin in vivo begins with the exposure of tissue factor, but the local accumulation of thrombin is also governed by the availability of procoagulant factors (including prothrombin), the exposure of negatively charged phospholipids on the platelet and other membrane surfaces, the washout rates of thrombin from its original site of generation, and the ability of coagulation inhibitors such as tissue factor pathway inhibitor and anti-thrombin to reach the site where thrombin and other coagulation factors are produced. Some coagulation proteins and inhibitors are contained within platelet α -granules and are eventually secreted at the site of platelet activation. Others are plasma-borne. To the extent that molecular transport becomes hindered in the region closest to the site of injury, secreted molecules will tend to accumulate and plasma-borne molecules will have difficulty gaining access. This means that as platelets begin to accumulate following vascular injury they participate not only by forming part of the hemostatic plug, but also by acting as obstacles to the free movement of molecules in the region closest to the injury.

Thus, we propose that regional differences in platelet activation and in thrombus structure are closely related to each other and are both the driver for and the consequence of regional variations in agonist distribution and packing density. The data presented here plus our earlier studies with the thrombin sensor highlight the overlap between the region of greatest packing density, slowest transport, and greatest thrombin activity.^{3,10} We have previously shown that the size of the thrombus shell is dependent on signaling downstream of platelet P2Y₁₂ receptors for ADP.³ At present, there is no way to detect ADP in vivo in real time. However, the vulnerability of the shell to P2Y₁₂ antagonists and the increase of shell size observed with a gain-of-function mutation in G₁₂ α ³ suggest that ADP concentration gradients extend further than do thrombin gradients. Therefore, it is a reasonable hypothesis that platelet recruitment initially establishes a shell-like thrombus that is converted to the transition zone and core by thrombin. In a sense, the emergence of greater packing density within the core helps to create a molecular prison for thrombin that, along with the presence of thrombin inhibitors, limits the size of the core and, therefore, the overall size of the thrombus. It is also reasonable to propose that differences in the

distribution of ADP and thrombin, as well as differences in the properties of the core and shell presage differences in safety and efficacy of P2Y₁₂ antagonists compared with PAR1 antagonists.

In conclusion, in the present studies we have developed a novel method for measuring intrathrombus solute transport in vivo and demonstrated for the first time that heterogeneities of protein transport and thrombus structure are critical regulators of thrombin distribution independent of other factors. We have also shown that changes in transport rates within the thrombus evolve in parallel with changes in platelet packing density, and that these changes are independent of α -granule exocytosis. In the 2 accompanying manuscripts,^{12,13} we use complementary experimental and computational approaches to test this model.

Acknowledgments

This work was supported by the National Institutes of Health, National Heart, Lung and Blood Institute (R01HL119070 and P01HL40387 [T.J.S. and L.F.B.] and R01HL103419 [S.L.D. and L.F.B.]) and the American Heart Association (11SDG5720011 [T.J.S.]). J.D.W., R.W.M., and M.T. were supported by National Institutes of Health training grant T32-HL07439.

Authorship

Contribution: J.D.W. designed and conducted the experiments, analyzed data, and wrote the manuscript; T.J.S. conducted experiments and analyzed data; R.V., R.W.M., and M.T. analyzed data and performed data modeling; and S.L.D. and L.F.B. analyzed data and wrote the manuscript.

Conflict-of-interest disclosure: The authors declare no competing financial interests.

The current affiliation for R.V. is Department of Chemical, Biological & Pharmaceutical Engineering, New Jersey Institute of Technology, Newark, NJ.

Correspondence: Lawrence F. Brass, Perelman School of Medicine, University of Pennsylvania, 815 BRB II/III, 421 Curie Blvd, Philadelphia, PA 19104; e-mail: brass@mail.med.upenn.edu.

References

- van Gestel MA, Heemskerk JW, Slaaf DW, et al. Real-time detection of activation patterns in individual platelets during thromboembolism in vivo: differences between thrombus growth and embolus formation. *J Vasc Res*. 2002;39(6):534-543.
- Hechler B, Nonne C, Eckly A, et al. Arterial thrombosis: relevance of a model with two levels of severity assessed by histologic, ultrastructural and functional characterization. *J Thromb Haemost*. 2010;8(1):173-184.
- Stalker TJ, Traxler EA, Wu J, et al. Hierarchical organization in the hemostatic response and its relationship to the platelet-signaling network. *Blood*. 2013;121(10):1875-1885.
- Hayashi T, Mogami H, Murakami Y, et al. Real-time analysis of platelet aggregation and procoagulant activity during thrombus formation in vivo. *PLoS Arch*. 2008;456(6):1239-1251.
- Xu Z, Chen N, Shadden S, et al. Study of blood flow effects on growth of thrombi using a multiscale model. *Soft Matter*. 2009;5:769-779.
- Savage B, Saldívar E, Ruggeri ZM. Initiation of platelet adhesion by arrest onto fibrinogen or translocation on von Willebrand factor. *Cell*. 1996;84(2):289-297.
- Nesbitt WS, Westein E, Tovar-Lopez FJ, et al. A shear gradient-dependent platelet aggregation mechanism drives thrombus formation. *Nat Med*. 2009;15(6):665-673.
- Kuijpers MJ, Munnix IC, Cosemans JM, et al. Key role of platelet procoagulant activity in tissue factor- and collagen-dependent thrombus formation in arterioles and venules in vivo differential sensitivity to thrombin inhibition. *Microcirculation*. 2008;15(4):269-282.
- Neeves KB, Diamond SL. A membrane-based microfluidic device for controlling the flux of platelet agonists into flowing blood. *Lab Chip*. 2008;8(5):701-709.
- Welsh JD, Colace TV, Muthard RW, Stalker TJ, Brass LF, Diamond SL. Platelet-targeting sensor reveals thrombin gradients within blood clots forming in microfluidic assays and in mouse. *J Thromb Haemost*. 2012;10(11):2344-2353.
- Wannemacher KM, Zhu L, Jiang H, et al. Diminished contact-dependent reinforcement of Syk activation underlies impaired thrombus growth in mice lacking Semaphorin 4D. *Blood*. 2010;116(25):5707-5715.
- Stalker TJ, Welsh JD, Tomaiuolo M, et al. A systems approach to hemostasis: 3. Thrombus consolidation regulates intrathrombus solute transport and local thrombin activity. *Blood*. 2014;124(11):1824-1831.

13. Tomaiuolo M, Stalker TJ, Welsh JD, Diamond SL, Sinno T, Brass LF. A systems approach to hemostasis: 2. Computational analysis of molecular transport in the thrombus microenvironment. *Blood*. 2014; 124(11):1816-1823.
14. Zhu L, Bergmeier W, Wu J, et al. Regulated surface expression and shedding support a dual role for semaphorin 4D in platelet responses to vascular injury. *Proc Natl Acad Sci U S A*. 2007; 104(5):1621-1626.
15. Leiderman K, Fogelson AL. The influence of hindered transport on the development of platelet thrombi under flow. *Bull Math Biol*. 2013;75(8): 1255-1283.
16. Leiderman K, Fogelson AL. Grow with the flow: a spatial-temporal model of platelet deposition and blood coagulation under flow. *Math Med Biol*. 2011;28(1):47-84.
17. Voronov RS, Stalker TJ, Brass LF, Diamond SL. Simulation of intrathrombus fluid and solute transport using in vivo clot structures with single platelet resolution. *Ann Biomed Eng*. 2013;41(6):1297-1307.
18. Kim OV, Xu Z, Rosen ED, Alber MS. Fibrin networks regulate protein transport during thrombus development. *PLoS Comput Biol*. 2013; 9(6):e1003095.
19. Muthard RW, Diamond SL. Blood clots are rapidly assembled hemodynamic sensors: flow arrest triggers intraluminal thrombus contraction. *Arterioscler Thromb Vasc Biol*. 2012;32(12):2938-2945.